HAL
open science

Coarsening and dendritic instability of spheroidal graphite in high silicon cast iron under thermal cycling in the ferritic domain

André Ebel, Mariana Alves Pegoraro, Benoît Malard, Christophe Tenailleau, Jacques Lacaze

To cite this version:

André Ebel, Mariana Alves Pegoraro, Benoît Malard, Christophe Tenailleau, Jacques Lacaze. Coarsening and dendritic instability of spheroidal graphite in high silicon cast iron under thermal cycling in the ferritic domain. Scripta Materialia, 2020, 178, 10.1016/j.scriptamat.2019.11.001 . hal-02363594

HAL Id: hal-02363594

https://hal.science/hal-02363594v1

Submitted on 14 Nov 2019

HAL is a multi-disciplinary open access archive for the deposit and dissemination of scientific research documents, whether they are published or not. The documents may come from teaching and research institutions in France or abroad, or from public or private research centers.

L'archive ouverte pluridisciplinaire **HAL**, est destinée au dépôt et à la diffusion de documents scientifiques de niveau recherche, publiés ou non, émanant des établissements d'enseignement et de recherche français ou étrangers, des laboratoires publics ou privés.

Coarsening and dendritic instability of spheroidal graphite in high silicon cast iron under thermal cycling in the ferritic domain

André EBEL[a,b], Mariana ALVES PEGORARO[a], Benoit MALARD[a], Christophe TENAILLEAU[a], Jacques LACAZE[a]

a CIRIMAT, Université de Toulouse, CNRS, France

b LCTS, Université de Bordeaux, France

Corresponding author: Jacques LACAZE

CIRIMAT, ENSIACET, BP 44362, 31030 Toulouse cedex 4, France

Tel.: +33534323415, e-mail: Jacques.lacaze@ensiacet.fr

Abstract

High silicon ferritic spheroidal graphite cast irons have been developed for high temperature service, in particular under thermal cycling conditions. The theoretical maximum service temperature is defined as the upper limit of the two-phase ferrite+graphite domain, which increases with the alloy silicon content. While isothermal heat treatment close to this temperature showed little evolution of the graphite distribution, thermal cycling led to a significant coarsening of the graphite particles associated with dendritic overgrowth of the large graphite particles. This unexpected behaviour is here observed and described for the first time.

Keywords

Cyclic heat treatment, dendritic growth, graphite, spheroidal graphite cast iron

Funding: none; conflict of interest: none.

Studies devoted to high temperature behaviour of ferritic cast irons have been concerned with oxidation resistance and mechanical properties. Because silicon is known to increase both oxidation resistance and the upper temperature of the domain where ferrite is stable, high-silicon spheroidal graphite cast irons (SGI) have been developed since the 1980s [1,2]. These alloys are used in many applications including loading under thermal cycling. Studies on the effect of thermal cycling on tensile properties [3,4] and on the thermomechanical behaviour [5,6] of high silicon SGI have been carried out with maximum temperature up to 800°C which is within the ferritic domain for the investigated alloys. These studies involved a limited number of cycles and the only changes in microstructure that were reported concerned oxidation of inclusions associated with the last-to-solidify areas and partial recrystallization of ferrite for the highest maximum temperatures (750°C and 800°C).

Investigating the behaviour of high-silicon SGI when submitted to a much higher number of thermal cycles is of interest as this may be more representative of the actual life cycle of industrial components. In order to do so, a material containing mainly 3.10 wt.% C, 4.45 wt.% Si and also 0.0037 wt.% Sb (balance Fe) was selected. Before casting, the melt was treated for graphite spheroidization and inoculated as described previously [7]. Metallographic observation showed a fully ferritic matrix in the as-cast state, with an even distribution of graphite spheroids as seen in figure 1-a. The surface number density of spheroids was 580 particles per mm^2 and the graphite fraction was about 0.1.

Two types of experiments were run on 10x20x2 mm^3 samples: isothermal heat treatment and cyclic heat treatment. Isothermal heat treatment was performed in a muffle furnace for 50 hours at 800°C. Thermal cycling was performed between 100°C and 800°C in a dedicated facility. In this facility, samples were hung to a holder which was cyclically introduced into a furnace pre-heated to 800°C, and then withdrawn from the furnace and fan-cooled before being heated up again. One of the samples had a thermocouple welded onto it for continuous control of the thermal cycles. The whole thermal cycle duration was 480 s, including 360 s of heating, 60 s of holding at 800±10°C and 60 s of cooling. Part of the samples were withdrawn for analysis after 1000, 2000 and finally 3000 cycles. This latter number of cycles was selected so that the time nominally spent at 800°C should be 50 hours.

Metallographic observations and 2D image analysis were performed on the bulk of the heat treated specimens which was not affected by surface oxidation and decarburization. Image analysis was carried out to quantify the evolution of the graphite volume fraction, particles number density and size distribution. Particle size was evaluated using an equivalent diameter D equal to $4 \cdot \frac{A}{P}$, where A and P are respectively the area and perimeter of a particle. Measurements were carried out on 10 micrographs taken along the centre of the sample section and then averaged.

Figure 1-b shows that isothermal heat treatment may result in a very slight coarsening of the graphite spheroids which was better evidenced by the number density of graphite particles (see below). In contrast, Figure 1-c shows that the microstructure of the sample after 3000

cycles presents a marked coarsening of the graphite particles which is associated with morphological instability of the largest growing particles.

It was observed that the number density of graphite particles decreased from 580 mm^{-2} for the as-cast sample to 520 mm^{-2} for the sample isothermally treated and to 470-500 mm^{-2} for the thermally cycled samples. These values confirm a slight coarsening process during isothermal treatment, and a stronger effect of thermal cycling.

The normalized size distributions of graphite particles size obtained after isothermal holding and after 1000, 2000 and 3000 cycles are compared to the initial distribution in the as-cast material in Figure 2. The relative distributions for the heat-treated samples are all similar, showing an increase in the number of 0-10 µm and 20-30 µm particles, and a decrease in the number of the 10-20 µm ones when compared to the as-cast sample distribution. More significantly, it is seen that thermal cycling leads to the increase in the number of particles with equivalent diameter higher than 30 µm. It is also clearly seen that the size of the largest particles increased from 30-40 µm in the as-cast state to more than 60 µm after 3000 cycles.

Coarsening of graphite particles has been reported in the case of heat-treatment at a temperature where austenite is stable but never when the matrix remains ferritic. In contrast to the case of austenite, the carbon content in ferrite is assumed so low that such a phenomenon has been generally considered as unexpected. However, in the present work, it was observed that the apparent fraction of graphite measured on 2D metallographic sections did significantly increase with cycling from 0.1 in the as-cast state to 0.17 after 3000 cycles. Measurements of the sample density showed a correlated decrease, from 6.9 g/cm^3 for the as-cast sample to 6.8, 6.6 and finally 6.4 g/cm^3 respectively after 1000, 2000 and 3000 cycles. This correlation means that cavities developed during cycling which were considered as graphite during image analysis because they had the same contrast on light optical micrographs. In other words, graphite particles did partly dissolve and carbon atoms were transferred to other locations in relation to coarsening.

In the present case, these cavities certainly developed first at the interface between graphite precipitates and the matrix, but then evolved into holes left by the small spheroids being dissolved during the coarsening process. Unfortunately, it was not possible to identify unambiguously these cavities on metallographic sections, as graphite particles may have also spalled off during sample preparation. To evaluate the actual possibility for graphite to dissolve during heat-treatment in the ferritic domain, the Fe-C isopleth section of the Fe-C-Si-Mn phase diagram at 4.45 wt.% Si and 0.25 wt.% Mn was drawn (Figure 3). It is seen that the carbon content in ferrite increases above 700°C, being about 0.012 wt.% at 800°C, while it is virtually zero at 700°C and below. It can thus be conjectured that this change in ferrite carbon content between 700°C and 800°C is instrumental in the coarsening process.

Figure 3 shows also that the lowest temperature of the ferrite/austenite/graphite three-phase field is 860°C, i.e. that a heat-treatment with a maximum temperature at 800°C should not lead to the appearance of austenite. However, because micro-segregation of silicon that has developed during solidification could have triggered partial transformation of ferrite to austenite, it appeared necessary to verify that there was no phase change in the studied

material during thermal cycling with an upper temperature of 800°C. Differential thermal analyses were thus run at 2, 5, 10 and 20°C/min (see supplementary information). The measured temperatures for the start of transformation upon heating, $T_{start\text{-}C}$, and for the end of transformation upon cooling, $T_{peak\text{-}R}$, were plotted versus the scanning rate. The values extrapolated to a zero scanning rate are 860°C upon heating and 840°C upon cooling, thus confirming that there is no phase change during thermal cycling when the maximum temperature is set at 800°C.

The most intriguing observation made during the present work was the characteristics of the protuberances developing on the largest spheroids. Figure 4 shows that after 2000 cycles they assume a dendritic shape protruding from the initial compact spheroids. The length of these protuberances goes up to 30-40 µm in figure 4. After 1000 cycles, it was observed that the protuberances have just started to develop while after 3000 cycles the coarsening process led to a thickening of the dendritic protuberances which often joined each other. In this latter case, areas of matrix were found isolated by graphite "arches" very similar to those described by Monchoux et al. [9]. Note that this latter study involved heating in the austenitic domain, while the present results demonstrate that graphite dissolution may take place without the ferrite to austenite transformation of the matrix.

Some hints for understanding the growth phenomenon could be gained by evaluating the extent of graphite dissolution upon heating from room temperature (RT) to 800°C. The carbon balance can be written as:

$$\rho^{iron} \cdot w_C^0 = \rho^g \cdot w_C^g \cdot g^g + \rho^\alpha \cdot w_C^\alpha \cdot g^\alpha \qquad (1)$$

where ρ^{iron} and w_C^0 are the density and carbon content of the alloy, ρ^φ, g^φ and w_C^φ are, respectively, the density, the volume fraction and the carbon content of phase φ (g: graphite; α: ferrite). This mass balance may be differentiated and, after rearrangement using $dg^\alpha = -dg^g$, one gets:

$$dg^g = -\frac{w_C^g \cdot g^g \cdot d\rho^g + \left(1 - g^g\right) \cdot \left(\rho^\alpha \cdot dw_C^\alpha + w_C^\alpha \cdot d\rho^\alpha\right)}{\rho^g \cdot w_C^g - \rho^\alpha \cdot w_C^\alpha} \qquad (2)$$

High temperature X-rays were conducted to evaluate the change in lattice parameter of ferrite in the temperature range from RT to 800°C. The expansion coefficient was found equal to $1.5 \cdot 10^{-5}$ °C^{-1}. Using the density of a cast iron containing 4.25 wt.% Si [10], ρ^α was evaluated at 7570 kg.m^{-3} at RT. With the above expansion coefficient, the ferrite density is evaluated as 7300 kg.m^{-3} at 800°C, and its average value $\overline{\rho}^\alpha$ between RT and 800°C could be set to 7435 kg.m^{-3}. The density of graphite ρ^g varies from 2262 kg.m^{-3} at RT to 2221 kg.m^{-3} at 800°C [11] and its average value $\overline{\rho}^g$ was set to 2240 kg.m^{-3}. From all these values, it can be concluded that the first and last terms of the numerator in the right-hand side of equation (2) are negligible. The average change Δg^g between RT and 800°C may thus be approximated as:

$$\Delta g^g \approx -\frac{\left(1-g^g\right)\cdot \overline{\rho}^{\alpha}\cdot \Delta w_C^{\alpha}}{\overline{\rho}^{g}\cdot w_C^{g}-\overline{\rho}^{\alpha}\cdot \overline{w}_C^{\alpha}} \quad (3)$$

According to figure 3, Δw_C^{α} was set at 0.012 wt.% and its average value $\overline{w}_C^{\alpha}$ at half of it. With these values and the graphite fraction g^g set to 0.1, the change in graphite fraction upon heating from RT to 800°C is about $\Delta g^g = -3.6\cdot 10^{-4}$ ($-3.6\cdot 10^{-2}$%). This change in graphite fraction may be converted into the size of the gap formed in between the graphite spheroids and the surrounding matrix upon heating from RT to 800°C. The 2D nodule count, N_A, given above, may be converted to the volume nodule count by $N_V = \frac{2}{\pi}\cdot\frac{N_A}{\overline{D}_2}$ [12], where $\overline{D}_2$ is the average diameter of the spheroids as measured on the 2D section. With $g^g = N_A\cdot\frac{\pi\cdot(\overline{D}_2)^2}{4}$, $\overline{D}_2$ could be set to 15 µm which gives $N_V \approx 24600$ mm^{-3}. The change in graphite fraction can then be written as $\Delta g^g = N_V\cdot 4\cdot\pi\cdot\overline{r}^2\cdot\Delta\overline{r}$, in which $\overline{r}$ and $\Delta\overline{r}$ are, respectively, the average radius and average change in radius of the graphite spheroids. This change in radius gives the size of the gap formed between the outer surface of graphite spheroids and the surrounding matrix when the upper temperature of 800°C is reached. By inserting the value of Δg^g evaluated above, one gets a gap size of $2.1\cdot 10^{-2}$ µm.

Though the above gap appears very small, it was readily realized that if this value could accumulate from one cycle to another it would sum up to 42 µm after 2000 cycles. As a matter of fact, this latter value appears very similar to the length of the protuberances seen in figure 4. This result thus suggests that the carbon dissolved during heating and holding at 800°C re-precipitated in preferred locations during cooling and not uniformly around the large particles. On the largest particles, reiterating this process leads to the protuberances illustrated in figure 4. Thermal cycling is thus essential for the development of these morphological instabilities, and this explains why they could not have appeared during isothermal heat-treatment.

Thermal cycling in the ferritic domain has been shown to dramatically decrease mechanical properties of spheroidal high-silicon cast irons [3,4,6]. However, none of these previous works reported a microstructure evolution as observed in the present work. In the case of the works by Lin et al. [3,4] this was certainly due to the maximum temperature they considered, either 700°C or 750°C, which may have been too low for graphite dissolution to take place. It appears more surprising that Cheng et al. [5] and Avery et al. [6] did not observe microstructure changes similar to those detailed here as the highest temperature that they investigated was also 800°C. This is probably because these authors were focused on the areas damaged by thermomechanical cycling, but this could as well be related to the very rapid cycles that they used, which may not have given enough time for graphite dissolution in the upper temperature range to occur.

Understanding the detailed mechanism leading to the morphological instabilities described here is certainly worthy of further investigation, as well as evaluating if they may play a role in the decrease of the mechanical properties of high silicon SGI under cyclic thermal loadings.

[1] W. Fairhurst, K. Röhrig, Foundry Trade J. 146 (1979) 657–681.

[2] L. Delin, R. Logan, G. Burger, G. Liao, D. McFarlan, B. Black, R. Williams, SAE technical paper 2007-01-12

[3] Hung-Mao Lin, Truan-Sheng Lui, Li-Hui Chen, Mater. Trans. 44 (2003) 173-180.

[4] Hung-Mao Lin, Truan-Sheng Lui, Li-Hui Chen, Mater. Trans. 44 (2003) 1209-1218 .

[5] C.P. Cheng, T.S. Lui, L.H. Chen, Metall. Mater. Trans. A 30A (1999) 1549-1558.

[6] K. Avery, Jwo Pan, C. Engler-Pinto, SAE Technical paper 2015-01-0557

[7] R. González-Martínez, U. de la Torre, J. Lacaze, J. Sertucha, Materials Science and Engineering A 712 (2018) 794-802.

[8] J.O. Andersson, T. Helander, L. Höglund, P.F. Shi, B. Sundman, Calphad 26 (2002) 273-312.

[9] J.P. Monchoux, C. Verdu, G. Thollet, R. Fougères, A. Reynaud, Acta mater. 49 (2001) 4355-4362.

[10] T. Matsushita, E. Ghassemali, A. Gomez Saro, L. Elmquist, A.E.W. Jarfors, Metals 5 (2015) 1000-1019.

[11] P. Dietrich, G. Lesoult, in "State of the art of computer simulation of casting and solidification processes", Les éditions de Physique, E-MRS, 1986, 225-235

[12] M. Coster, J.L. Chermant, Précis d’analyse d’images, Presses du CNRS, 1989

Figure captions

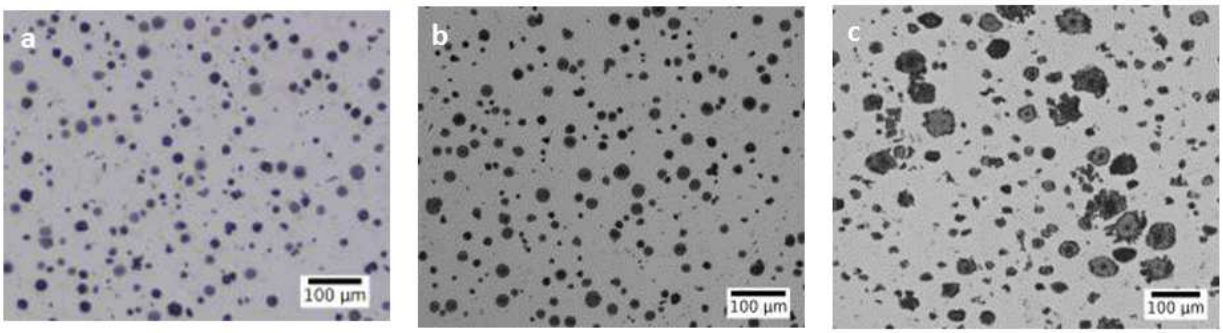

Figure 1 – Optical micrographs of the alloy in the as-cast state (a), after isothermal treatment of 50 h at 800°C (b), and after 3000 thermal cycles (c).

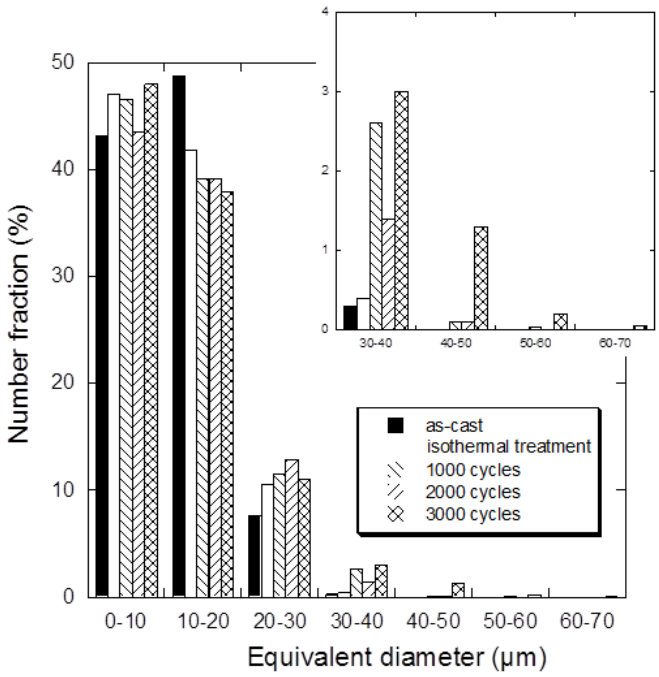

Figure 2 – variation of the normalized number distribution of 2D equivalent diameters of the graphite particles after isothermal holding at 800°C and after 1000, 2000 and 3000 thermal cycles, as compared to the distribution in the as-cast material. The insert corresponds to a zoom in the domain of particles larger than 30 µm in equivalent diameter. The maximum observed standard deviation was ±10% of the value shown for any of the classes.

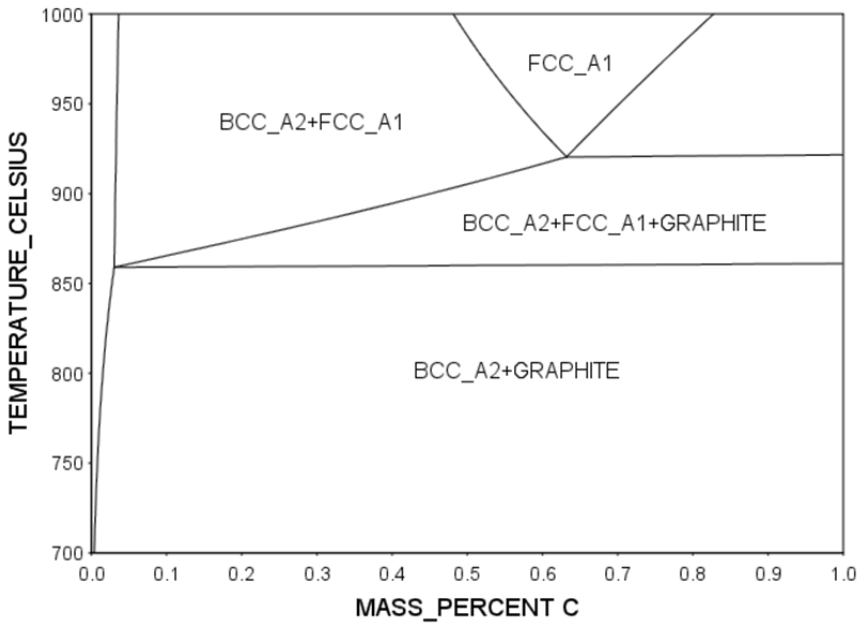

Figure 3 – Isopleth Fe-C section of the Fe-C-Si-Mn phase diagram at 4.45 wt.% Si and 0.25 wt.% Mn showing that ferrite (BCC_A2) is stable up to a temperature of 860°C where austenite (FCC_A1) appears. The calculations were made with the Thermocalc software and using the TCFE8 database [8].

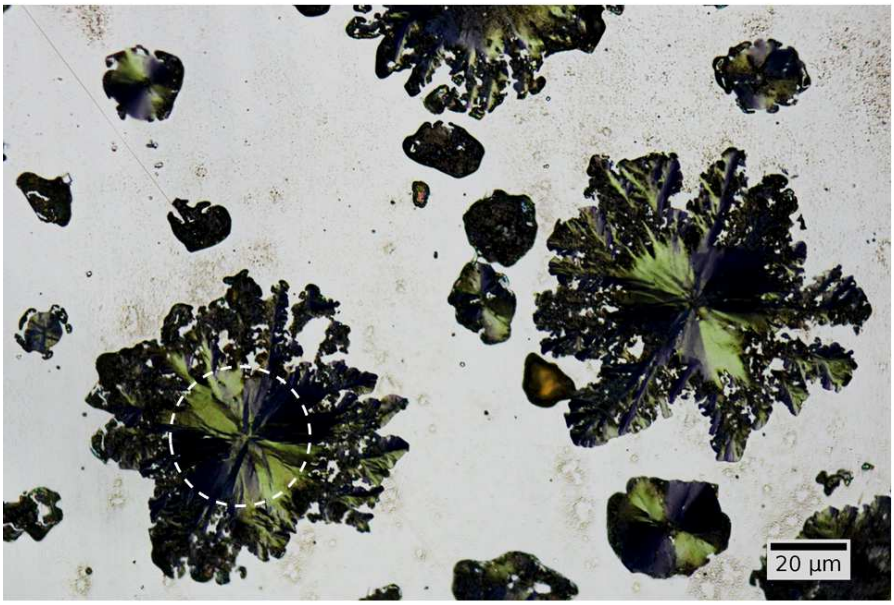

Figure 4 – Optical micrograph (polarized light) of dendritic protuberances observed on the sample having been submitted to 2000 thermal cycles. The white dashed circle superimposed on the nodule to the left defines the central compact part of the nodule which is considered as its original outer surface. The extensions out of this circle are thus the protuberances grown during thermal cycling.